Prepared for submission to JCAP

The Maximum Circular Velocity Dependence of Halo Clustering

Contents

1 Introduction **1**

2 The Simulation **1**

3 The Maximum Circular Velocity Dependence of Halo Clustering **2**
3.1 The Maximum Circular Velocity 2
3.2 Samples 2
3.3 Halo Bias 3

4 Applications **6**
4.1 Mvir-based v.s. Vmax-based 6
4.2 $\Delta\Sigma(r)$ 6

5 Discussion **7**

1 Introduction

The halo model has been remarkably successful in describing observations of galaxy clustering. In particular, the Halo Occupation Distribution (HOD) and the Conditional Luminosity Function (CLF) have been widely used to constrain not only the galaxy-halo connection [XXX] but also cosmology [XXX]. The fundamental assumption in both formalisms is that galaxy occupation statistics only depends on halo mass.

The spatial distribution of dark matter (DM) halos in N-body simulations, however, exhibits dependence on halo mass as well as on additional properties such as halo formation time [XXX]. The dependence of halo clustering upon other properties besides halo mass known as halo assembly bias. There have been several studies showing the correlation between halo formation time and environment, and therefore any other properties which depends on formation time or environment (such as concentration, spin, and velocity anisotropy) affect to the assembly bias. This assembly bias violates the standard HOD/CLF assumption and also questions how these model can predict the clustering statistics of galaxies correctly.

As a response to halo assembly bias, recent trend in the way to populate galaxies has been to use the Abundance Matching technique based on the maximum circular velocities of halos. The motivation behind use of the maximum circular velocity is that it depends only on the central part of the halo potential (i.e., potentially more closely related to galaxy formation) and sets early in the growth of the halo [XXX: Frank's paper] (i.e., more robust to disruption in mergers).

In this paper, we explore the dependence of galaxy clustering on the central velocity dispersion both on small and large scales. We show that some of the features on small scales in a detailed halo model come from the effects of back-splash halos, which is one of the categories of halos classified based on the halo merger tree.

2 The Simulation

We use cosmological N-body simulations called the Bolshoi simulation and the MultiDark simulation, described in XXX and XXX respectively, to investigate the maximum circular velocity dependence of halo clustering. The Bolshoi simulation uses 2048^3 particles with a volume of $(250h^{-1}\mathrm{Mpc})^3$, while the MultiDark simulation uses the same number of particles as the Bolshoi simulation but with a volume of $(1h^{-1}\mathrm{Gpc})^3$. Both simulations assumes a flat ΛCDM model with density parameters $\Omega_m = 0.27$, $\Omega_\Lambda = 0.73$, $\Omega_b = 0.0469$, and $\sigma_8 = 0.82$, $n = 0.95$, $h = 0.70$. The details of the simulations are described in XXX. We use both simulations to get a large dynamic mass range.

For halo identification, we use the ROCKSTAR halo finder (XXX) where the halo masses and maximum circular velocities are computed from bound particles. For the sake of the internal structure of halos to be resolved well enough, we make a conservative cut in mass and maximum circular velocity. We use halos whose mass is greater than $10^{12}h^{-1}\mathrm{M}_{\odot}$ (corresponding to > 100 particles per halo) and whose maximum circular velocity is greater than 200km/s for the MultiDark simulation, and halos whose mass is greater than $10^{11}h^{-1}\mathrm{M}_{\odot}$ (corresponding to > 740 particles per halo) and whose maximum circular velocity is greater than 95km/s for the Bolshoi simulation. Those values correspond to the peak in the number of halos by binning them as a function of mass and maximum circular velocity.

From the merger tree, we can classify halos into three different categories: host halo, subhalos, and ejected halos. Host halos are the halos which have never been within the virial radius of more massive halos. Subhalos are the halos which are within the virial radius of more massive halos at $z = 0$. Ejected halos, sometimes called "backsplash" halos, are the distinct halos at $z = 0$ whose main progenitors passed through the virial radius of a more massive halos at least once in the past. In later sections, when we say halos without any specifications, we include both host halos and ejected halos.

3 The Maximum Circular Velocity Dependence of Halo Clustering

In this section, we investigate the maximum circular velocity dependence of halo clustering on both large and small scales. We first start with an analytic expression of the maximum circular velocity computed from the halo mass and its concentration. Then, we explain how we select halos for each sample to remove the halo mass dependence using the analytic expression of the maximum circular velocity. Finally, we show how halo biases differ for those samples both on large scales and small scales.

3.1 The Maximum Circular Velocity

In order to compute the maximum circular velocity for halos, we assume that dark matter halos are defined as a spherical halo with a virial radius. Those halos have average density equal to $\Delta_{\mathrm{h}}\rho_{\mathrm{crit}}$ where $\Delta_{\mathrm{h}} = 360$ for the MultiDark and Bolshoi simulations. We also assume that those spherical halos have an NFW density profile (XXX). Then, the maximum circular velocity $\overline{V}_{\mathrm{max}}$ as a function of the halo mass M_{vir} and its concentration c is given by:

$$\overline{V}_{\mathrm{max}} = 0.465 M_{\mathrm{vir}}^{1/3} \sqrt{G(\frac{4}{3}\pi\Delta_{\mathrm{h}}\rho_{\mathrm{crit}}\Omega_m)^{1/3}\frac{c}{\ln(1+\mathrm{c}) - \mathrm{c}/(1+\mathrm{c})}}. \tag{3.1}$$

The median concentration-mass relation at $z = 0$ obtained from the Bolshoi simulation in Ref. XXX(Klypin et al. 2011) is:

$$\log_{10}c = -0.097\log_{10}\mathrm{M}_{\mathrm{vir}} + 2.148. \tag{3.2}$$

By using the above median concentration to Eq. 3.1, we obtain a one to one mapping between the virial halo mass and its maximum circular velocity, denoted as $\overline{V}_{\mathrm{max}}$ hereafter. Given this mapping, we can translate clustering measurements as a function of halo mass into predicted clustering measurements as a function of maximum circular velocity. Our goal below is to determine whether this conversion describes the measured clustering or if there is a residual dependence on the maximum circular velocity.

3.2 Samples

We first split the sample into a sequence of virial mass bins, chosen such that there are the same numbers of halos in each bin. This process is reminiscent of an abundance matching procedure (cite XXX). We then further split each bin into two subsamples with their observed $V_{\mathrm{max,obs}}$ greater than (denoted by "upper") or less than (denoted as "lower") $\overline{V}_{\mathrm{max}}$. Fig. 1 shows the distribution of halo mass and maximum circular velocity classified into "upper" (blue dots) and "lower" (green dots) samples as an example. Note that the number of halos in "upper" and "lower" subsamples are almost equal for any halo mass bins. This selection ensures that both the upper and lower subsamples have

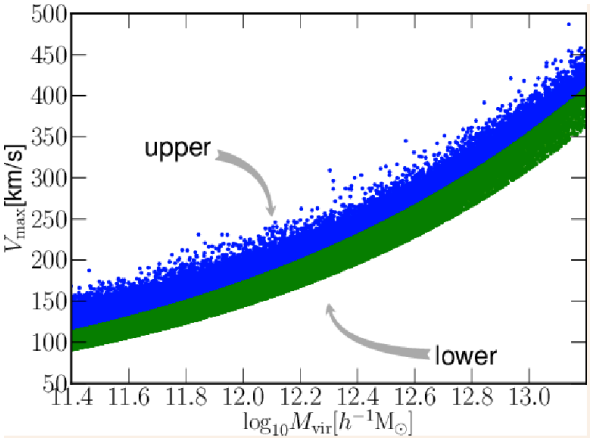

Figure 1. Distribution of halo mass and maximum circular velocity at $z = 0.0$ for halos from the Bolshoi simulation. The blue dots represent halos whose observed maximum circular velocity, $V_{\rm max,obs}$, is greater than $\overline{V}_{\rm max}$, while the green dots are the ones with smaller $V_{\rm max,obs}$ than $\overline{V}_{\rm max}$. The boundary between blue and green dots correspond to $\overline{V}_{\rm max}$ computed from Eq. 3.1.

the same mean halo mass. Therefore, in the absence of an additional $M_{\rm vir}$ dependence on clustering, these samples should have the same clustering properties. Note that this would not be true if we had simply split the sample along $V_{\rm max}$, since the two resulting subsamples would have different mean halo masses.

3.3 Halo Bias

In order to measure halo biases, we first compute halo-matter cross correlation functions for each subsample. We use cross correlation functions to reduce the shot noise effect on the error. Here, instead of using full DM particles, we subsample 10^6 particles to compute the cross correlation functions and matter auto correlation functions. Then, we define a linear bias:

$$b_{\rm lin} = \sum_i (\xi_{hm}(r_i)/\xi_{mm}(r_i))/N_{\rm bin}, \tag{3.3}$$

where ξ_{hm} and ξ_{mm} are halo-matter and matter-matter correlation functions and we take the average of the ratio on r from $10h^{-1}$Mpc to $20h^{-1}$Mpc, which contains 20 bins in total.

Fig. 2 shows linear biases as a function of halo mass by splitting each sample into "upper" and "lower" subsamples. For large halo masses, the "lower" subsamples have larger linear biases than the "upper" subsamples. This result is consistent with the result discusses in Ref. XXX(Dalal et al. 2008). For low halo masses, the "upper" subsamples have larger linear biases than the "lower" subsamples. Those halos which have larger maximum circular velocities than $\overline{V}_{\rm max}$ are the ones which are supposed to grow into larger mass halos, but somehow the mass growth is suppressed. This is why those halos in the "upper" subsamples cluster more strongly than the ones in the "lower" subsamples. As halo mass decreases, the difference in linear bias between the "upper" and "lower" subsamples increases up to $\sim 40\%$. On low mass end, there is a drop in the ratio of the linear biases. We think that the drop is due to mass resolution of the simulation.

Although halo biases are constant on large scales, halo biases on small scales are scale-dependent (XXX:reference). We explore whether the "upper" and "lower" subsamples have different scale-dependence in small scale halo biases. In order to explore that, we take the ratio of the cross correlation functions between the "upper" and "lower" subsamples and normalize it with their linear biases. Fig. 3 shows the ratios for several mass bins. The first three mass bins labeled in the figure, $\log_{10}{\rm M}[{\rm h}^{-1}{\rm M}_\odot] = 11.7, 12.0, 12.2$, are from the Bolshoi simulation, and the last two mass bins, $\log_{10}{\rm M}[{\rm h}^{-1}{\rm M}_\odot] = 12.7, 13.1$, are from the MultiDark simulation. The "upper" and "lower" subsamples have very different scale-dependence, especially around 1 to $2h^{-1}$Mpc. Furthermore, the difference

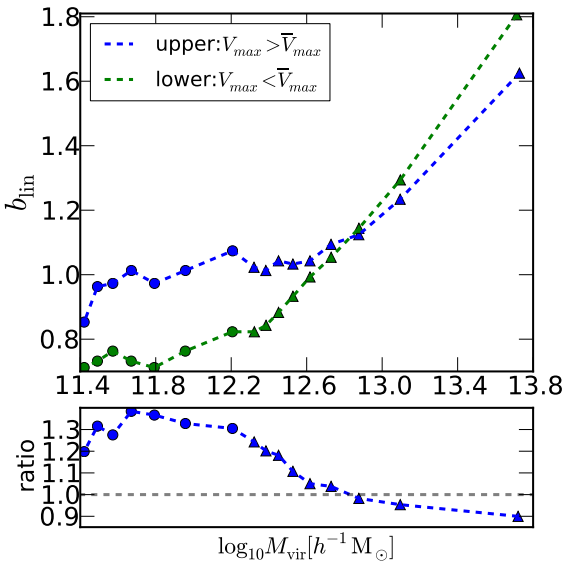

Figure 2. Upper panel: Linear bias at $z = 0.0$ as a function of halo mass from the Bolshoi simulation (circle points) and the MultiDark simulation (triangle points). The blue circles corresponds to a linear bias for halos whose maximum circular velocities are greater than $\overline{V}_{\rm max}$ (called "upper" samples in the text), while the green circles correspond to halos whose maximum circular velocities are smaller than $\overline{V}_{\rm max}$ (called "lower" samples). Lower panel: Ratio of linear biases between "upper" (i.e., $V_{\rm max} > \overline{V}_{\rm max}$) and "lower" (i.e., $V_{\rm max} < \overline{V}_{\rm max}$) samples from the Bolshoi simulation and the MultiDark simulation. As halo masses decrease, the difference on linear bias between "upper" and "lower" samples becomes larger up to 40%. .

on small scales becomes larger for lower halo mass samples. This implies that those low mass halos in the "upper" subsamples cluster strongly and likely to live in hot environments near massive halos.

Up to now, we use both host halos and ejected halos to compute halo biases. Both types of halos are identified as distinct halos at $z = 0$. Ejected halos, however, are halos which were identified as a part of a more massive halos at one or more occasions in the past. Those ejected halos tend to exist around a more massive halos (any reference?), and only some of them may be gravitationally bound to other more massive halos. Therefore, the efect on the scale-dependent biases may be caused by those ejected halos. To test this, we compute halo-matter cross correlation functions without the ejected halos. Similar to Fig. 2, we first compare linear biases as a function of halo mass. We observe that the ratios of linear biases between the "upper" and "lower" subsamples are suppressed by $\sim 10\%$. Next, we compare cross correlation functions on small scales, as shown in Fig. 4, similar to what was done in Fig. 3. Fig. 4 only shows the results for low mass halos from the Bolshoi simulation. This is because we do not find many ejected halos in the MultiDark simulation due to its mass resolution. Once the ejected halos have been removed, the deviation of the halo bias on small scales is greatly reduced. This implies an intimate connection between assembly bias and subhalo back-splashing.

We conclude that halos which have different $V_{\rm max}$ cluster differently even when those halos have the same virial mass. In particular, the scale-dependence of halo biases on small scales is significantly different, which is mainly caused by the ejected halos.

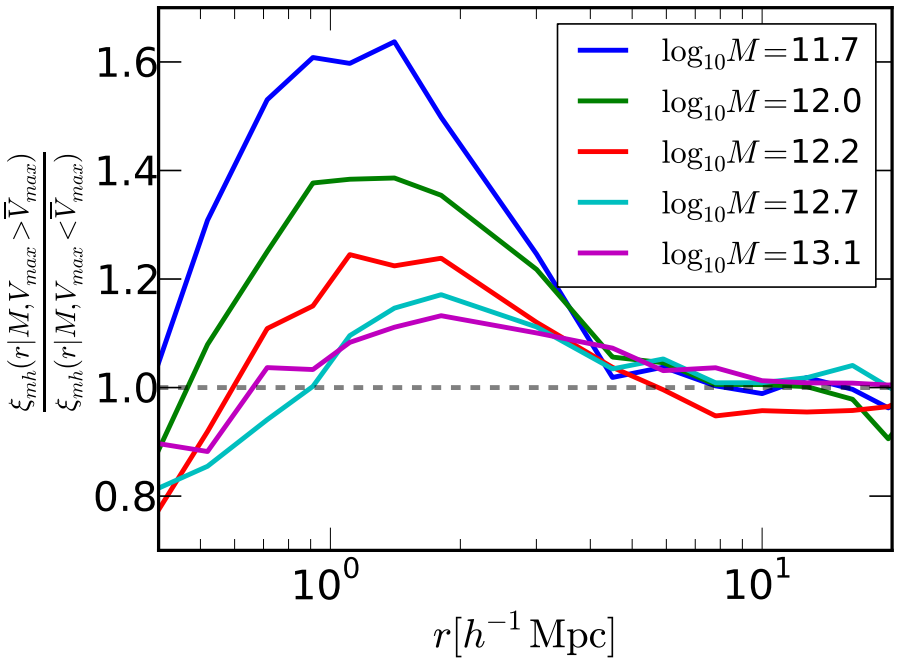

Figure 3. Ratio of halo-matter cross correlation functions between "upper" and "lower" subsamples normalized by their linear biases. The plots are from the Bolshoi simulation and the MultiDark simulation at z = 0.0. Each line corresponds to different halo mass bins labeled in the plots. Those plots show that "upper" and "lower" subsamples have different scale-dependence on small scales and the relative scale-dependence between those subsamples increases smoothly with decreasing halo mass. which lines come from MD...

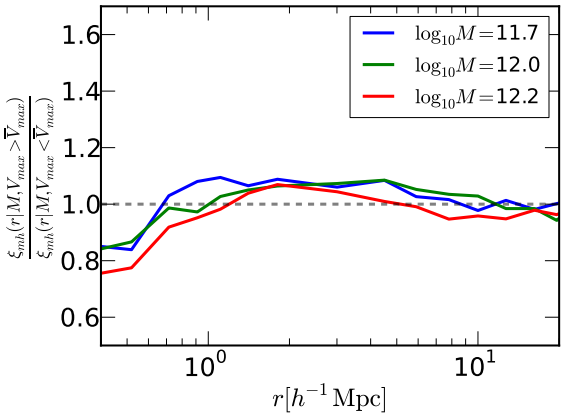

Figure 4. The same figures as Fig. 3 without ejected halos only from the Bolshoi simulation. As can be seen by comparing these results to those in Fig. 3, the $V_{\rm max}$-dependence of halo bias on small scales is dramatically reduced by excluding ejected subhalos. This implies an intimate connection between assembly bias and subhalo back-splashing.

–use jackknife sampling to put error bars

4 Applications

In this section, we demonstrate possible observational relevances of the results in the previous section to complement the halo theory results. We start with the abundance matching (citation?) technique based on halo mass and the maximum circular velocity, and then compute $\Delta\Sigma$(R) using those two different abundance matching techinique.

4.1 Mvir-based v.s. Vmax-based

In abundance matching, we link galaxy populations to halo populations by assuming that big galaxies live in big halos in a hierarchical manner. The question is what "big" halos really means. To rank order halos, we want to identify what kind of physical properties characterize halo "size". As a first step, we explore how the abundance matching based on halo mass and maximum circular velocity influence halo clustering.

Similar to the previous section, we compute halo-matter cross correlation functions for the abundance matched samples by splitting halos into a sequence of halo mass bins, $\overline{n}(M_{\rm vir})$, and the maximum circular velocity bins, $\overline{n}(V_{\rm max})$, chosen such that each bin has the same number of halos. We observe that when we include ejected halos, the linear biases for the $V_{\rm max}$-samples are larger than the ones for the $M_{\rm vir}$-samples by 5%, while the difference in linear biases is suppressed to 2% by excluding ejected halos. This result is consistent with the result in Sec. 3.2. The magnitude of the difference, however, is smaller than the cases of splitting the samples based on $\overline{V}_{\rm max}$.

We also compare the cross correlation functions on small scales. Figure 5 displays data in the same way as Figure 3 with the ejected halos on the left and without the ejected halos on the right. When those samples contain ejected halos, the $V_{\rm max}$-samples show very different scale-dependence on halo bias than the $M_{\rm vir}$-samples do. This scale-dependent feature becomes stronger as halo mass decreases. Without ejected halos, the difference on small-scale biases between the $M_{\rm vir}$- and $V_{\rm max}$-samples is reduced to $\sim 5\%$, which is the same order of magnitude as the case of Sec. 3.3 shown in Fig. 4.

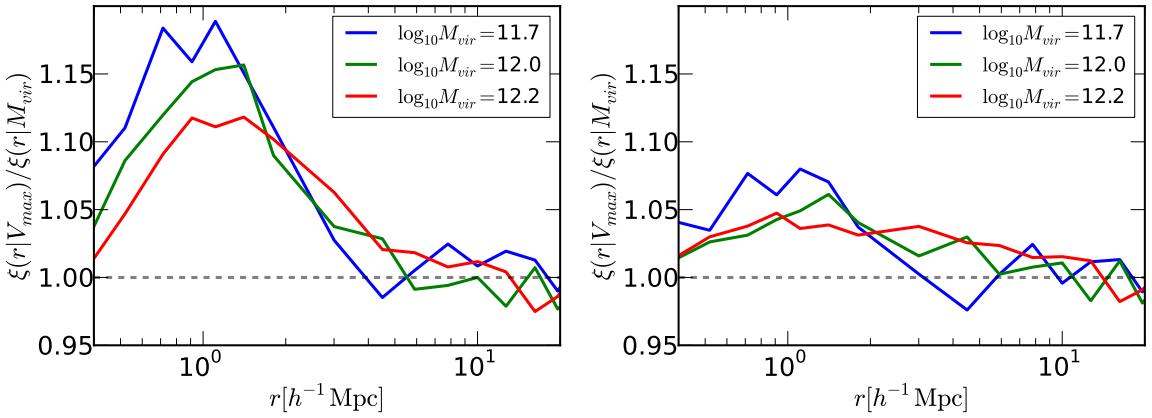

Figure 5. Ratio of halo-matter cross correlation functions between$M_{\rm vir}$-based and $V_{\rm max}$-based abundance matching samples with ejected halos (left) and without ejected halos (right). The ratios are normalized by their linear biases. Each line corresponds to different halo mass bins labeled in the plots. With ejected halos, the halo biases computed from the $V_{\rm max}$-samples have very different scale-dependence than the ones from the $M_{\rm vir}$-samples. By removing those ejected halos, the difference is more or less removed.

4.2 $\Delta\Sigma(r)$

–Select a bin of Milky Way mass host halos, and select their number-density-matched Vmax-selected equivalent. Use Peter Behroozi's stellar-to-halo mass relation to estimate the stellar mass of the central galaxy that would be found in these halos, then plot the halo-matter cross-correlation as a function of scale, over-plotting the two results.

–want to show: We show that the galaxy-galaxy lensing signal of low-mass centrals is impacted at the xxx-yyy% level, in a highly scale-dependent fashion, by the theoretical choice to empirically connect stellar mass to either host halo Vmax or Mvir.

5 Discussion